Some ideas

S.Bottoni, F.Galtarossa, A.Goasduff, A.Gottardo, D.Mengoni, M.Rocchini and the GAMMA collaboration

Marco La Cognata, ASFIN collaboration

T.Oishi RIKEN

INFN
Istituto Nazionale di Fisica Nucleare

The $^{26}Al^{gs}(n,p)^{26}Mg$ and $^{26}Al^{gs}(n,\alpha)^{23}Na$ reactions studied via the THM.

Spokespersons:
M. La Cognata, D. Mengoni, A. Caciolli

Contact person: F. de Oliveira

INFN
Istituto Nazionale di Fisica Nucleare

The $^{26}Al^{ms}(n,p)^{26}Mg$ and $^{26}Al^{ms}(n,\alpha)^{23}Na$ reactions studied via the THM.

Spokespersons:
M. La Cognata, D. Mengoni, A. Caciolli

Contact person: F. de Oliveira

INFN
Istituto Nazionale di Fisica Nucleare

Astrophysical background

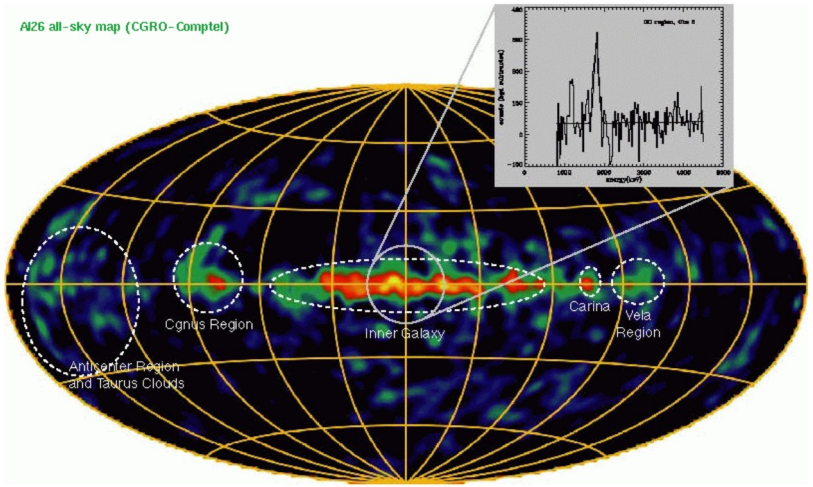

Observation of 1808.65 keV γ-rays from the decay of ^{26}Al to ^{26}Mg in the interstellar medium demonstrated that ^{26}Al **nucleosynthesis does occur in the present Galaxy.** The present-day equilibrium mass of ^{26}Al was found to be 2.8±0.8 M_{sun}.

The irregular distribution of ^{26}Al emission seen along the plane of the Galaxy provided the main argument for the idea that **massive stars** dominate the production of ^{26}Al. (Diehl et al 2006)

In CAIs (the oldest solid of the Solar System):
the inferred $6.5 \times 10^{-5} < (^{26}Al/^{27}Al)_0 < 2 \times 10^{-6}$.
^{26}Al was injected into the ^{26}Al-poor protosolar nebula, possibly by a wind from a neighboring massive star. **Crucial role in planets formation?**

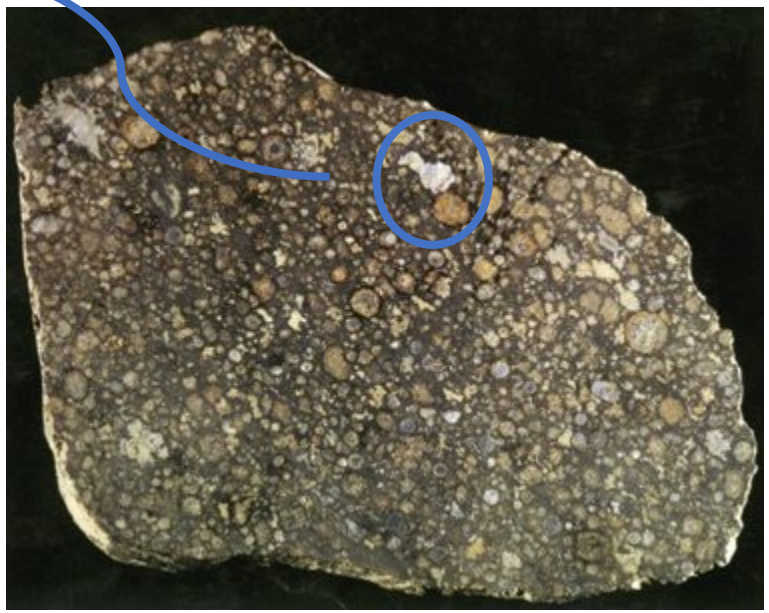

Presolar grains:
Corundum, hibonite and carbonaceous chondrites formed before the birth of the solar system show excesses in ^{26}Mg. The highest ratios are found in grains originated in supernova ejecta, but the largest number of grains with $^{26}Al/^{27}Al > 3 \times 10^{-3}$ (at least 100 times larger than the solar value) are of the type that come from **low mass stars**.

Status of the art

THE ASTROPHYSICAL JOURNAL SUPPLEMENT SERIES, 193:16 (23pp), 2011 March

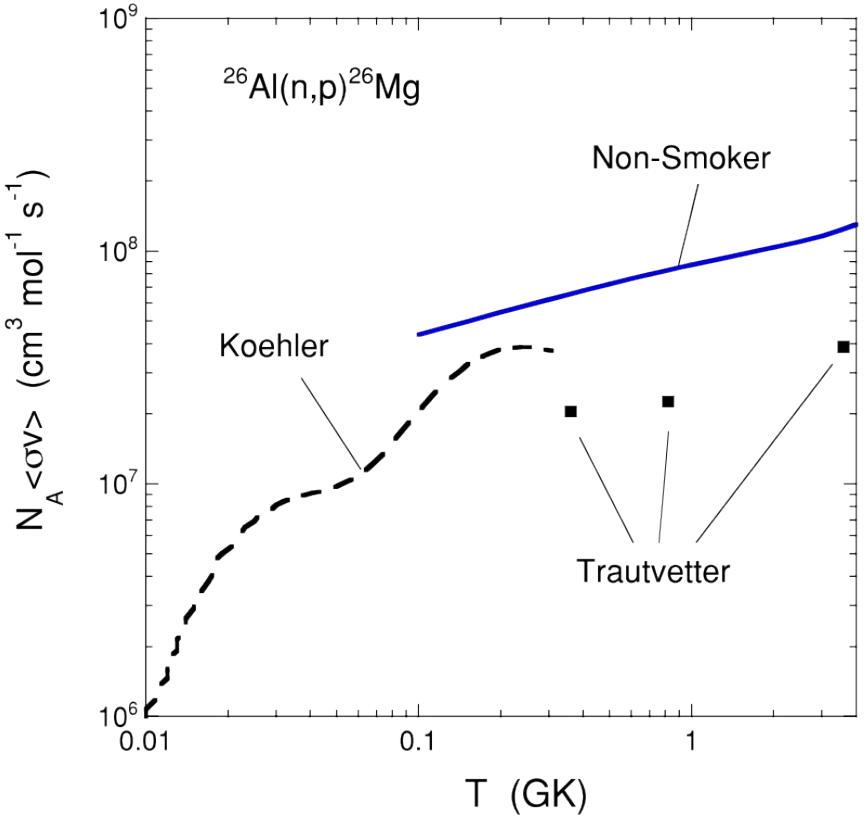

Figure 16. Reaction rates for ^{26}Al(n, p)^{26}Mg: dashed line, Koehler et al. (1997); blue solid line, Rauscher & Thielemann (2000); and squares (Trautvetter et al. 1986). The first (experimental) rate only takes the transition to the first excited state in ^{26}Mg into account, while the third (experimental) rate represents the combined transitions to the ground and first excited states in ^{26}Mg. The second rate is estimated using the Hauser–Feshbach theoretical model and includes transitions to all possible final states. Note that for this comparison only, the rates represent "laboratory rates," i.e., they do not account for thermal target excitations.

Temperatures of interest -> No experimental data available

- 1.1 GK (convective shell C/Ne burning)

Reaction[b]	Rate Multiplied By					
	100	10	2	0.5	0.1	0.01
^{26}Al^g(n,p)^{26}Mg	0.017	0.16	0.63	1.3	1.9	2.0
^{26}Al^g(n,α)^{23}Na	0.12	0.54	...	...	...	...
^{26}Al^m(n,p)^{26}Mg	0.58	...	...	...	...	...

- 2.3 GK (explosive Ne/C burning)

Reaction[b]	Rate Multiplied By					
	100	10	2	0.5	0.1	0.01
^{26}Al^g(n,p)^{26}Mg	0.017	0.14	0.57	1.6	2.9	3.8
^{26}Al^g(n,α)^{23}Na	0.21	0.54	...	...	...	...
^{26}Al^m(n,p)^{26}Mg	0.36	...	...	...	...	...
^{26}Al^m(n,α)^{23}Na	0.79	...	...	...	...	...

- 0.05 – 0.5 GK (AGB stars)
  - Large discrepancy between available data sets

Variation of the 26Al abundance for different changes in the rates

Theoretical approach

When narrow resonances dominate the S-factor the reaction rate can be calculated by means of the resonance **strengths and resonance energies only**. Both can be deduced from the THM cross section. Let's focus on resonance strengths

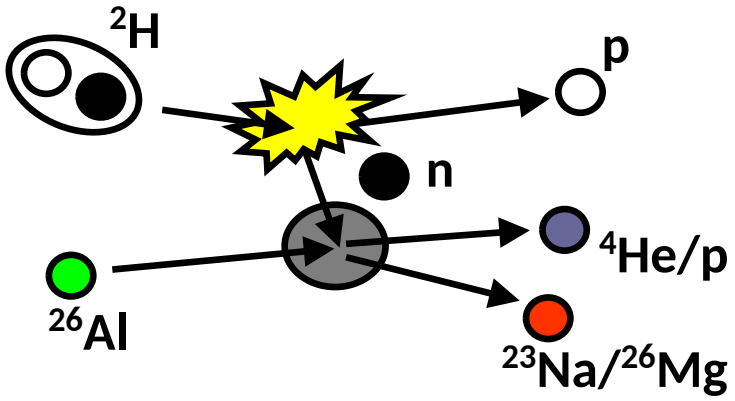

Trojan Horse Method: THM

$$(\omega\gamma)_i = \frac{\hat{J}_i}{\hat{J}_n \hat{J}_{^{26}Al}} \frac{\Gamma_{(n^{26}Al)_i}(E_{R_i})\,\Gamma_{(p^{26}Mg)_i}(E_{R_i})}{\Gamma(E_{R_i})}$$

What is its physical meaning?
Area of the Breit-Wigner describing the resonance

Where:
- $\hat{J}=2J+1$
- $\Gamma_{(AB)}$ is the partial width for the A+B channel
- Γ_i is the total with of the i-th resonance
- E_{Ri} is the resonance energy

Advantage:
no need to know the resonance shape (moderate resolution necessary)

In the THM approach:

$$(\omega\gamma)_i = \frac{1}{2\pi}\omega_i N_i \frac{\Gamma_{(n^{26}Al)_i}}{\frac{d\sigma_{d(^{26}Al,^{27}Al)p}}{d\Omega_n}}$$

Where:
- $\omega_i = \hat{J}_i / \hat{J}_p\,\hat{J}_{27Al}$ statistical factor
- N_i = THM resonance strength

Advantages:
- possibility to measure down to zero energy
- No need of expensive neutron beam facilities
- No spectroscopic factors in the $\Gamma_{(p27Al)}/\sigma$ ratio

However:
- QF condition must be enforced
- **Normalization necessary!!!!**

Previous examples (proof of principle)

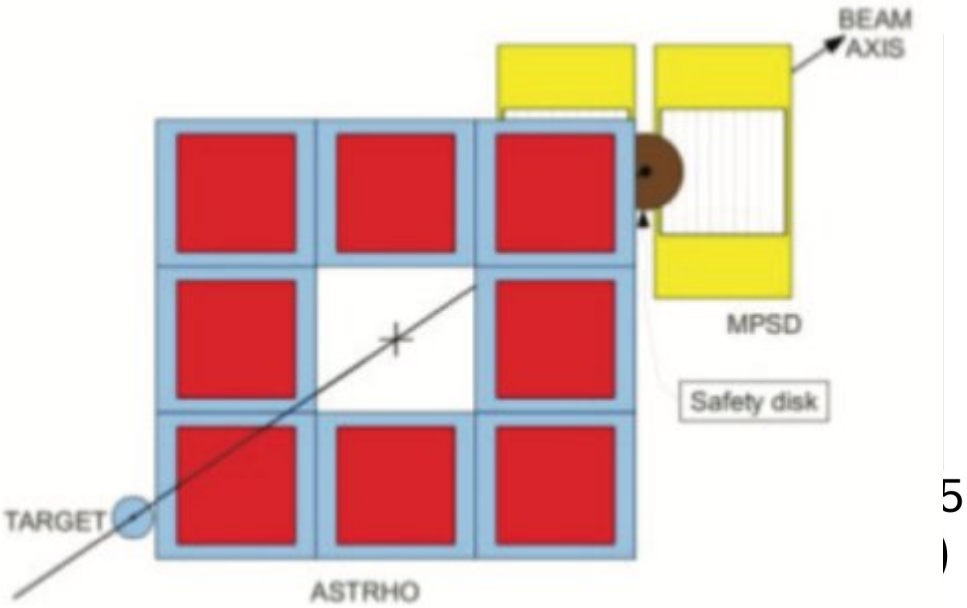

[Gulino et al. LNS report 2013-2014 arxiv.org1210.8269v1]

Measurement carried out at RIKEN, Japan, by using the ^{18}F beam provided by the CRIB **in-flight** facility, impinging on a CD2 target.
Resolution achieved: 120 keV FWHM
Analysis ongoing: many resonances in the $^{18}F(n,\alpha)^{15}N$ observed

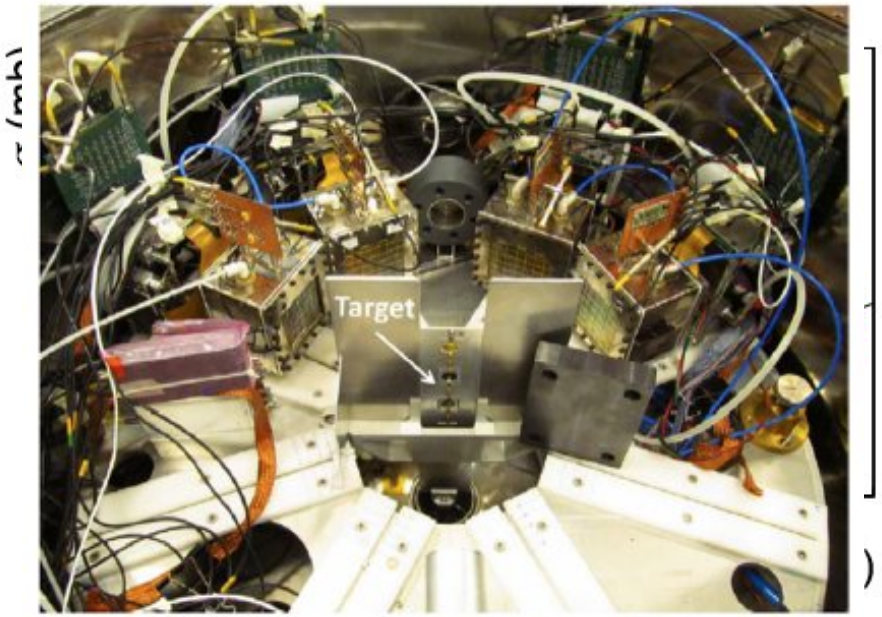

[Lamia et al. The Astrophysical Journal 879 (2019) 23]

Measurement carried out at LNL, Italy, by using the ^{7}Be beam provided by the EXOTIC **in-flight** facility, impinging on a CD2 target.
Resolution achieved: 300 keV FWHM
Very good agreement with existing data and improved uncertainty

Simulated experimental spectra

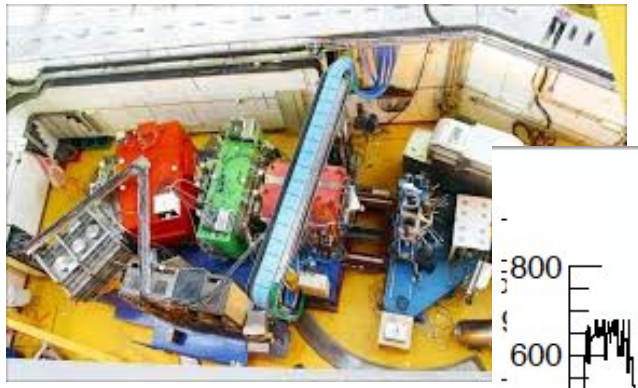

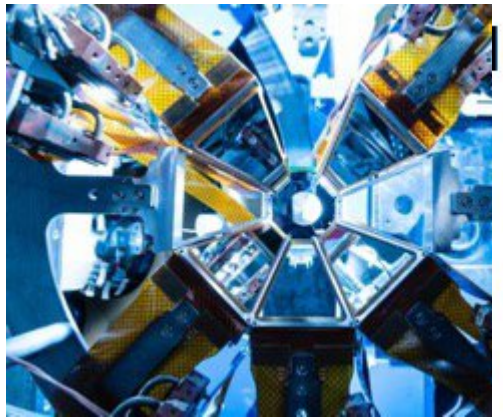

AGATA + VAMOS + M

Thanks to Guangxin Z
the simulations

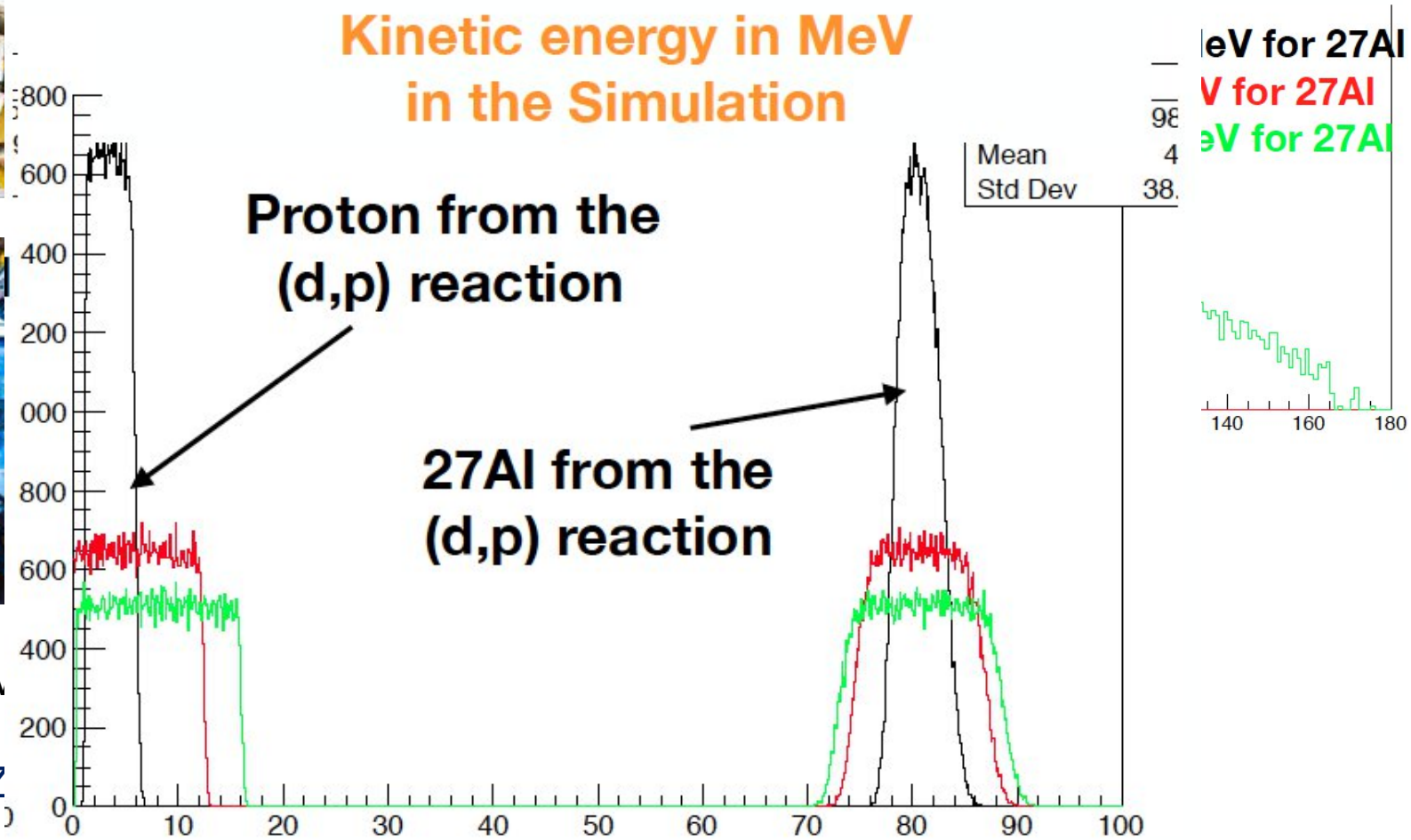

Data analysis

From $^{16}O(^{20}Ne,\alpha^{28}Si)\alpha$

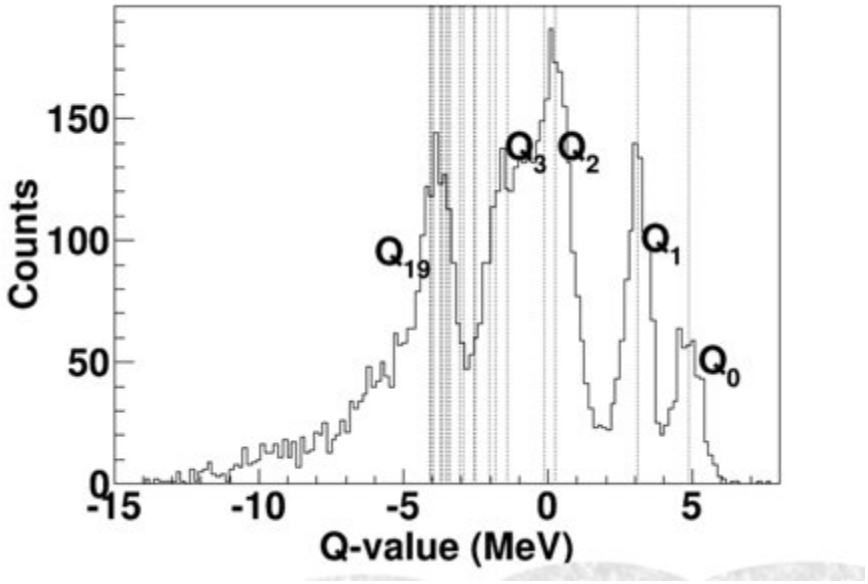

3 main steps are undertaken

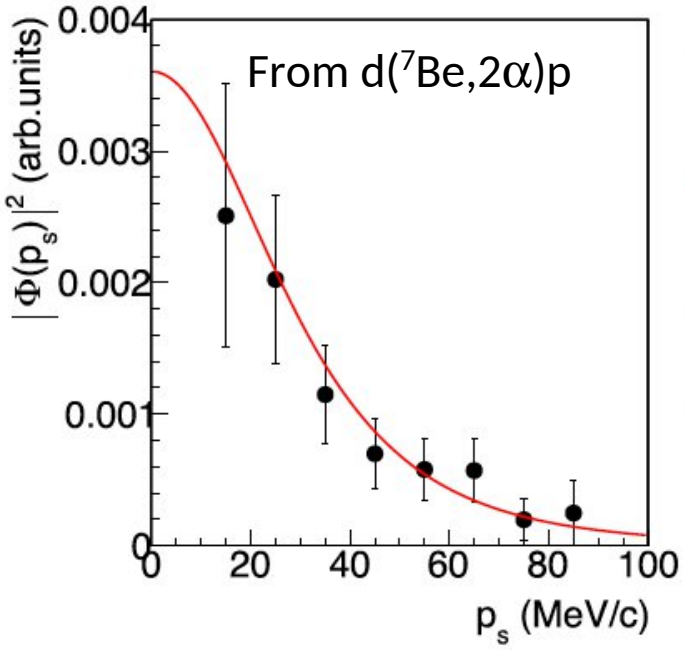

For the worse case:
7/2- resonance in ^{27}Al populated through ^{26}Al gs (black) and ^{26}Al isomeric state (red)

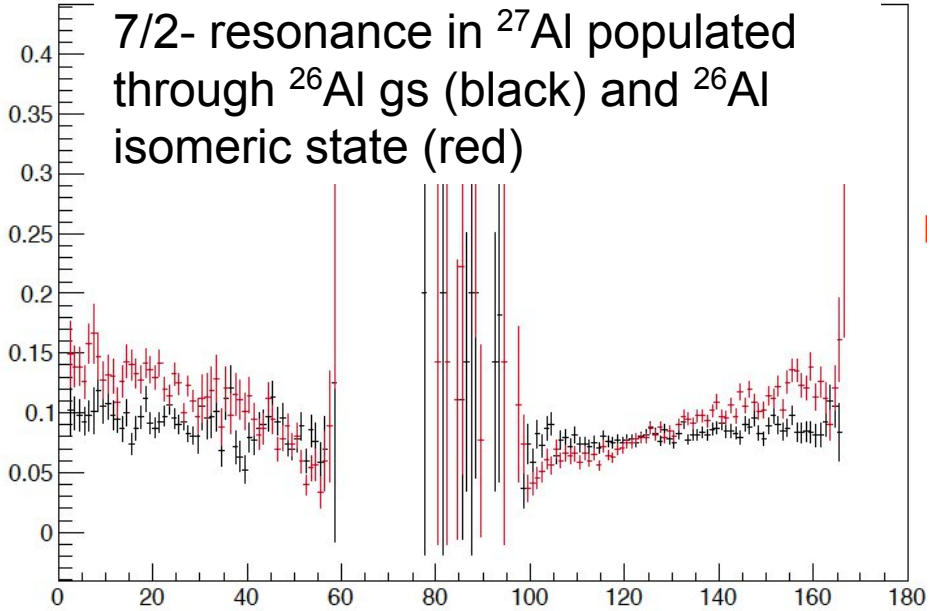

Channel selection: we need to separate the d(^{26}Al^{gs},p^{26}Mg)p (same for α+^{23}Na) from other channels

- PID through ΔE-E technique, TOF and Q-value selection
- ^{26}Mg excited states can be disentangled using the Q-value

Selection of the reaction mechanism: we deduce the proton momentum distribution and compare it with theoretical one. If the process is QF, then the theoretical one is the same as inside deuteron

Extraction of the cross section:

- Extraction of angular distribution (possibility to separate gs from isomeric thanks to ΔJ=5) and integration
- Normalization to direct data

Experimental setup

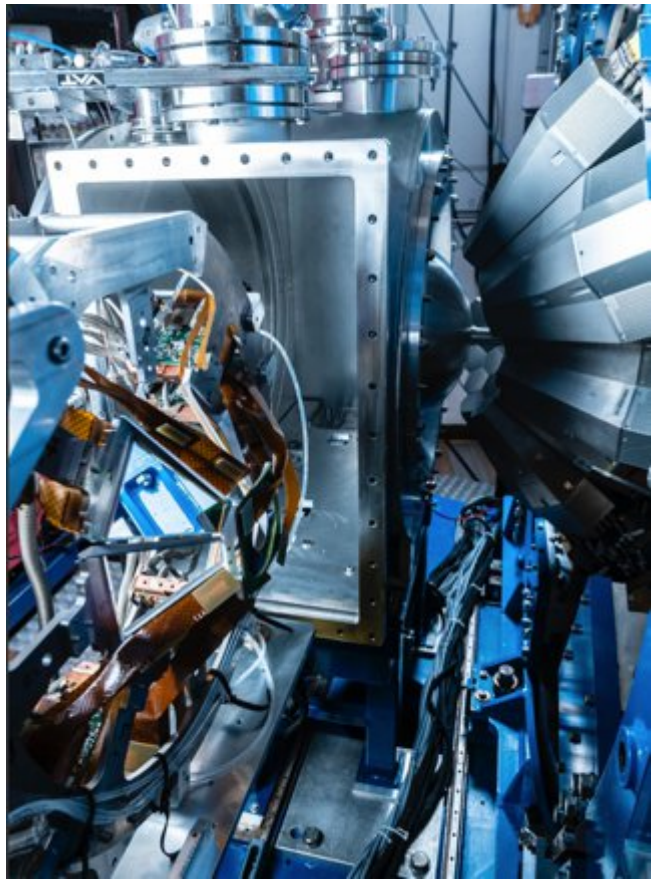

- GRIT: angular distribution and E_{Ex}
- VAMOS: channel sel./background, Doppler correction
- AGATA: cross-section contribution to individual excited state

- Beam intensity request:
- **~5x10^5 pps**
- Target 100 μg/cm^2 CD_2

VAMOS

- COMMENT IN THE PAC REPORT: Z separation or ToF ?

- After discussing with the locals it seems that both can be achieved under the condition:

- ~30 mb pressure in IC
- Removal of beam tracking detectors (CATS) → ToF between VAMOS focal plane and silicon (already achieved in the former experiments). Tof allows to separate low-energy particles stopped in the MUST2 DeltaE (20% of the total)

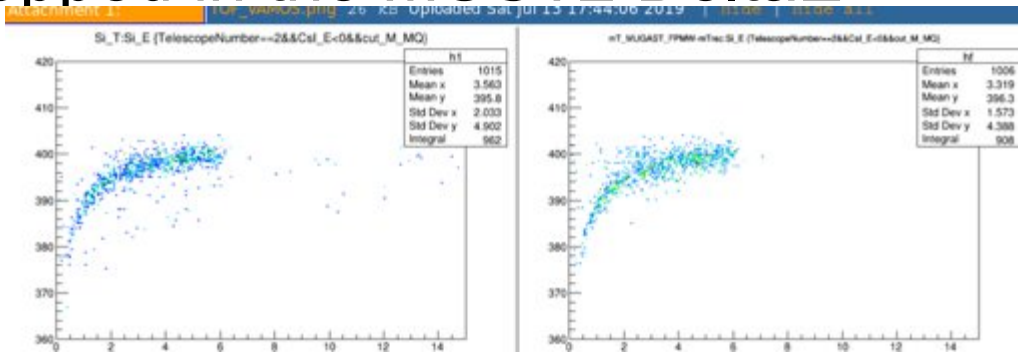

Final consideration & Beam time request

- Beam test (in case of PAC endorsement)
- Beam time: 8 days (in case of successful test)

Why the experiment should be carried out at GANIL?

- ✓ Need of ^{26}Al beam of intensities around 5x10^{5} pps
- ✓ Need of measurements at very small angles to catch the emitted ^{26}Mg (^{23}Na) fragment (important from channel selection)
- ✓ Possibility to catch ^{26}Mg and ^{23}Na : two measurements at the same time
- ✓ Possibility to weight different ^{26}Mg (^{23}Na) excited states
- ✓ Broad angular coverage necessary to reconstruct angular distributions (for accurate spectroscopy)

Backup slides

Extra slides 1: comparison of existing data

PHYSICAL REVIEW C **76**, 045804 (2007)

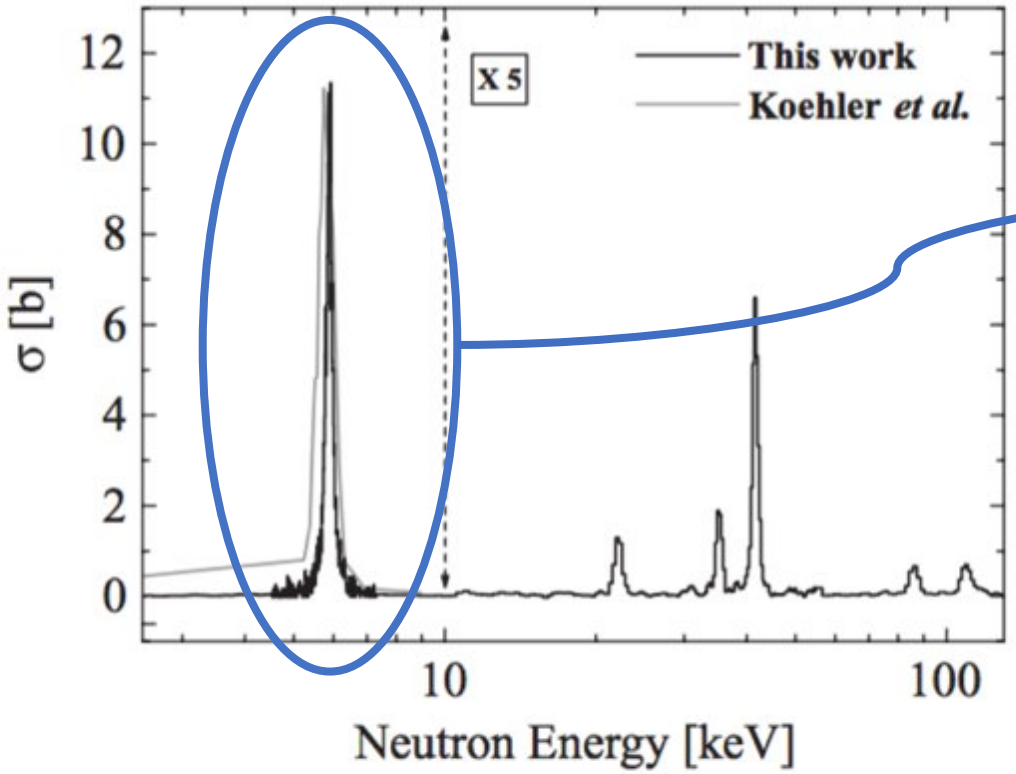

FIG. 5. ^{26}Al$(n, \alpha_0 + \alpha_1)^{23}$Na cross section determined in this work (black line) compared with the ^{26}Al$(n, \alpha_0)^{23}$Na cross section obtained by Koehler *et al.* [11] (gray line).

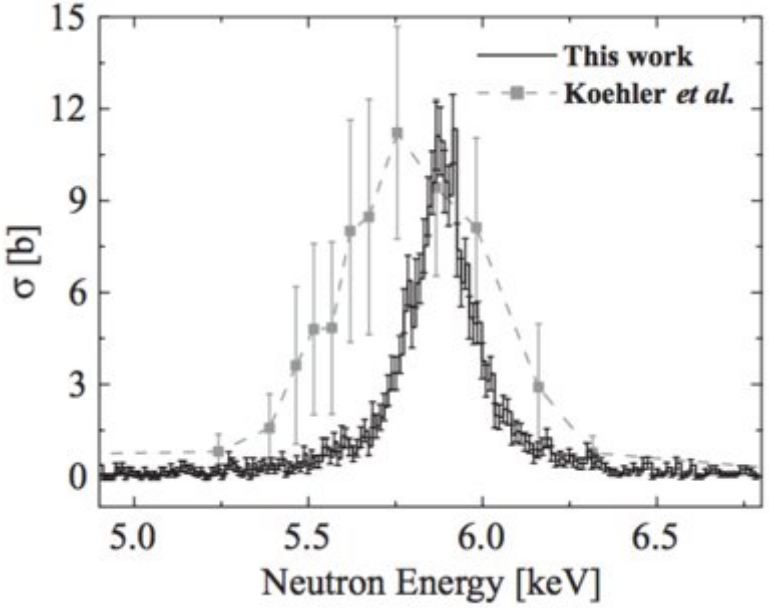

Two data sets available at low energies, showing large discrepancy.

- Koehler *et al.* (1993)
- De Smet *et al.* (2007)

The MACS from the latter work s have to be considered as lower limits for kT above 22 keV

Extra slides 2: application of THM

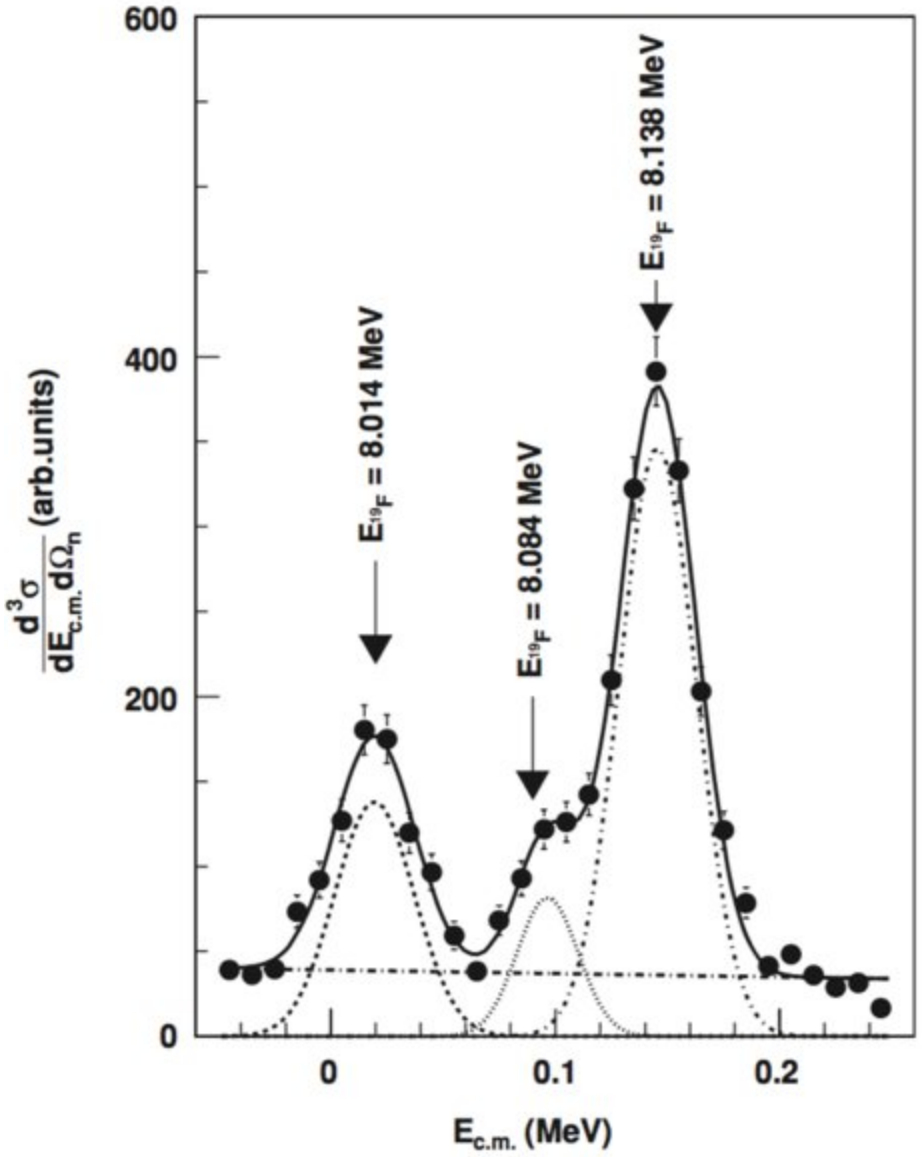

THE ASTROPHYSICAL JOURNAL, 708:796–811, 2010 January 1 doi:10.1088/0004-637X/708/1/796

A NOVEL APPROACH TO MEASURE THE CROSS SECTION OF THE $^{18}O(p,\alpha)^{15}N$ RESONANT REACTION IN THE 0–200 keV ENERGY RANGE

After extracting the resonance energies and strengths the reaction rate was calculated using the standard formula:

$$R^i_{^{18}O(p,\alpha)^{15}N} = N_A \langle \sigma v \rangle_{R_i}$$
$$= N_A \left(\frac{2\pi}{\mu k_B}\right)^{3/2} \hbar^2 (\omega\gamma)_i T^{-3/2} \exp(-E_{R_i}/k_B T),$$

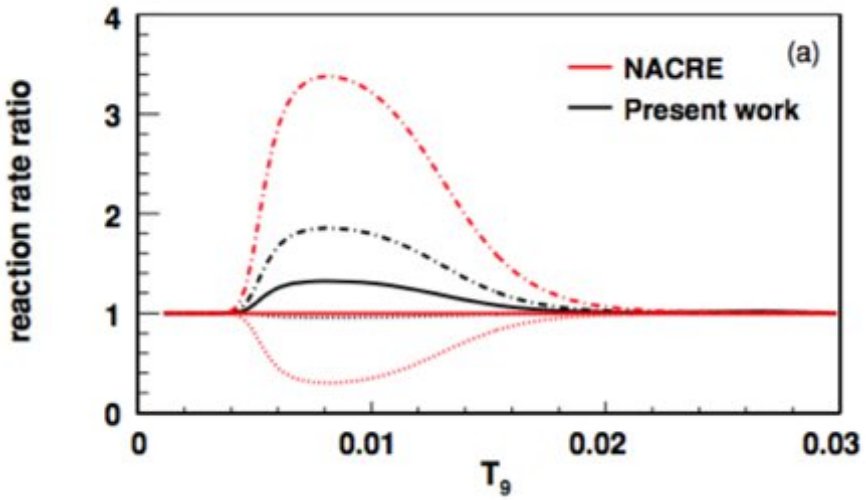

Very significant reduction in the uncertainty affecting the reaction rate at very low temperatures thanks to the **observation** of the 20 keV resonance

Extra slides 3: MACS

In the case of reactions induced by neutrons the reaction rate is replaced by MACS:

$$\langle \sigma \rangle = \frac{2}{\sqrt{\pi}} \frac{1}{(kT)^2} \int_0^{+\infty} \sigma(E_\mu) E_\mu e^{-\frac{E_\mu}{kT}} dE_\mu$$

that can be expressed in terms of resonance areas:

$$\langle \sigma \rangle = \sigma_{\text{th}} \sqrt{\frac{0.0253}{kT}} + \frac{2}{\sqrt{\pi}} \frac{1}{(kT)^2} \sum_{\text{res}} A_{\text{res}} E_{\text{res}} e^{-\frac{E_{\text{res}}}{kT}}$$

that is linked to resonance strength:

$$\omega_\alpha = \frac{k_{\text{res}}^2}{2\pi^2} A_{\text{res}}$$

For n-induced reactions an approach similar to the one developed for charged particles can be used. In THM, the transferred particles is a “quasi neutron” since the Coulomb barrier is overcome in the entrance channel.

Extra slides 4: use of three variables

Let's work in 2D for simplicity. We consider the d(^{26}Al,p^{26}Mg)p

From energy conservation:

$$E_{^{26}Al} + Q = E_{p_1} + E_{p_2} + E_{^{26}Mg}$$

From momentum conservation

$$p_{^{26}Al} = p_{p_1}\cos\theta_{p_1} + p_{p_2}\cos\theta_{p_2} + p_{^{26}Mg}\cos\theta_{^{26}Mg}$$

$$0 = p_{p_1}\sin\theta_{p_1} + p_{p_2}\sin\theta_{p_2} + p_{^{26}Mg}\sin\theta_{^{26}Mg}$$

Measured quantities: θ_{p2}, θ_{26Mg}, E_{p2}, E_{26Mg}

Known quantities: E_{26Al}

We have 3 equations and three unknown quantities, namely Q, θ_{p1} and E_{p1} ☾ extraction of Q value spectrum

If a single peak in Q value spectrum: I can fix Q and deduce E_{26Mg} from the system above

Extra slides 5: Detection setup

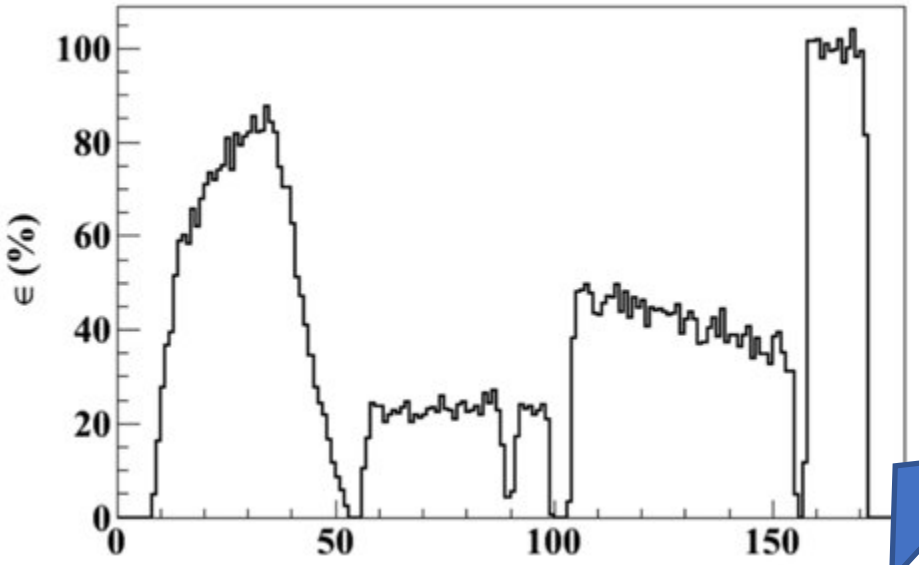

The geometrical angular efficiency of the proposed MUGAST configuration as a function of the polar angle.

Simulated energy spectra and Vamos acceptance:
if the Brho value is set as 0.575 Tm which is optimized for 26Mg13+ with the energy of 3.4 A MeV (black line) and the acceptance of magnetic is 10% in Brho (the region between the red lines), different charged particles with specific energy between two red curves can be transported by the beam line.

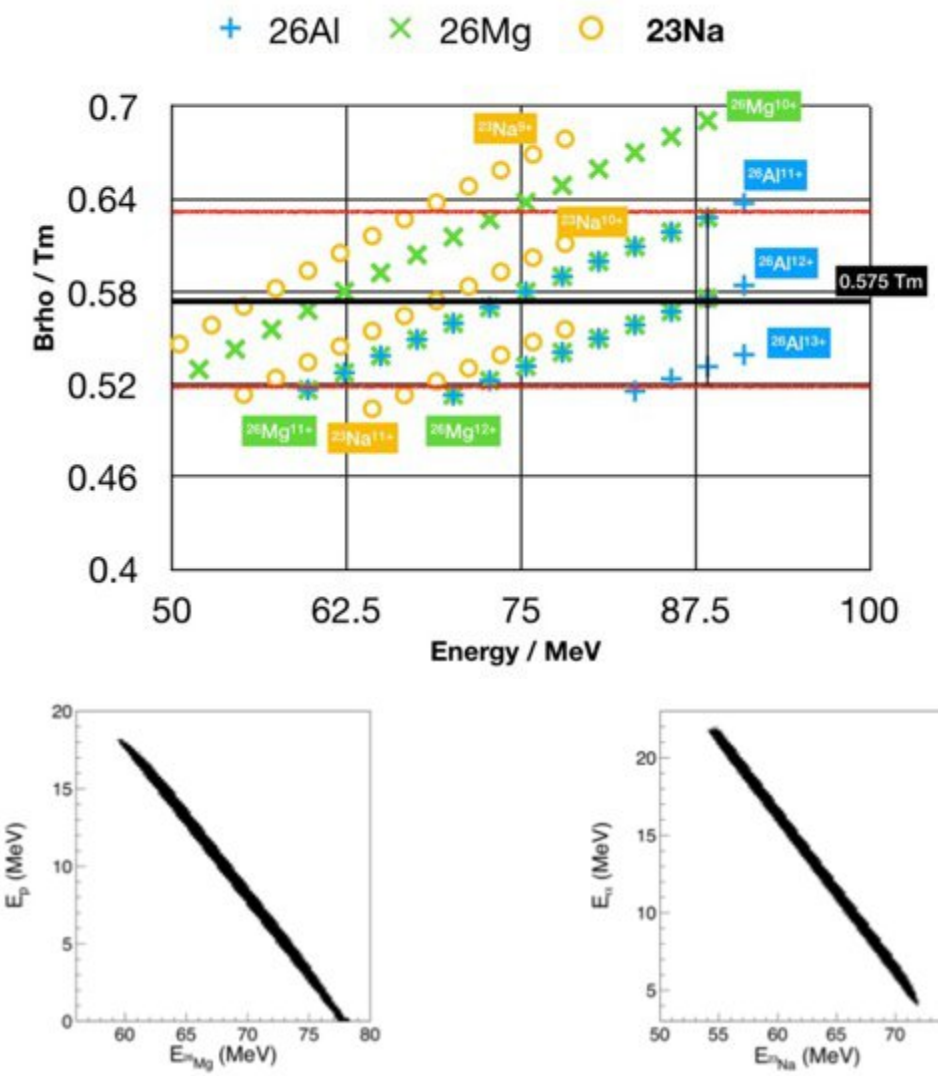

Figure 3: Energy correlation plots for the expected reactions, (n,p) and (n,α), on the left and right side, respectively.

The $^{21}Na(p,\alpha)^{18}Ne$ Time-Reversed reaction at TRIUMF

TUDA @ ISAC-II : CH2 targets ~ 300 and 500 μg/cm^2, ^{21}Na beam ~ 10^6 pps, Ebeam = 4 – 5.5 MeV

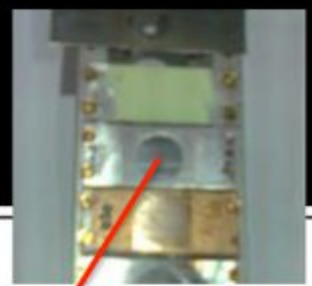

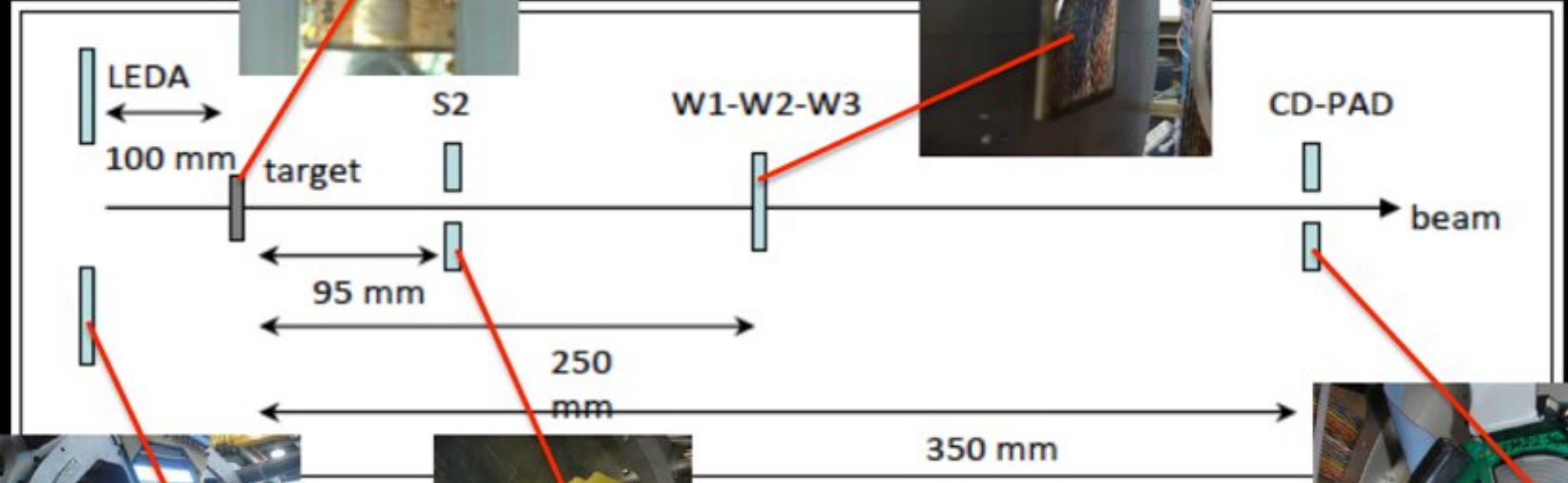

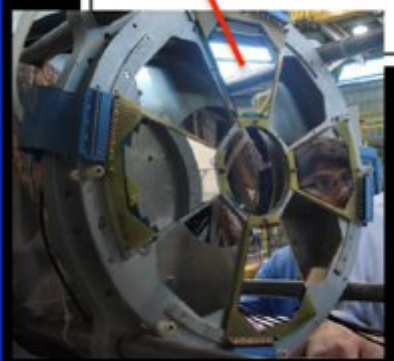

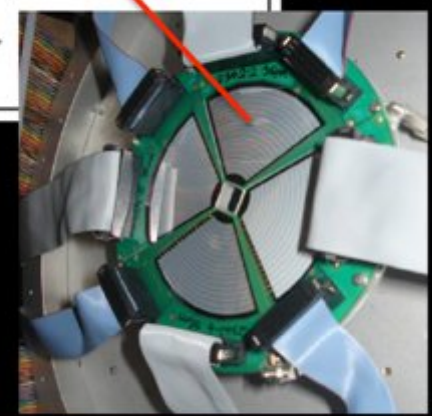

On the 2p spin entanglement

T. Oishi,

RIKEN Nishina Center, Nuclear Many-body Theory Laboratory

Two-proton (2p) radioactivity

Two-proton emission

- ✓ Observed in 2000.
- ✓ Radioactive decay by emitting two protons.
- ✓ From the Z=even parent nuclei in the proton-rich side.
- ✓ In the “true” 2p emission, so-called diproton correlation could exist.

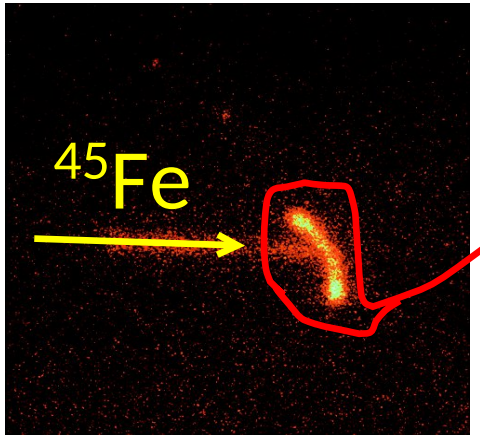

Are they entangled?

Di-nucleon (S_{12}=0, T_{12}=1) correlation

- ✓ Clustering of two neutrons or protons. Note that 2n/2p cannot be bound in vacuum.
- ✓ By the nuclear pairing force around the surface of the core nuclei, i.e., in the dilute-density region.
- ✓ Only theoretical predictions.

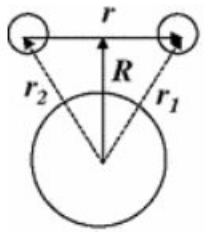

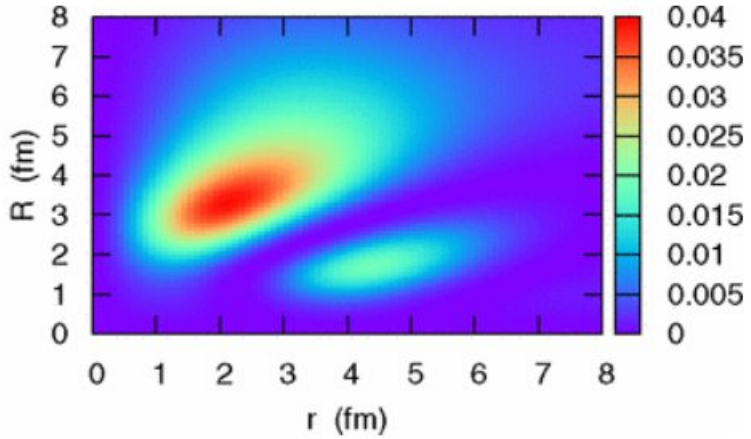

Can two nucleons become “entangled” ? ☾ Yes.

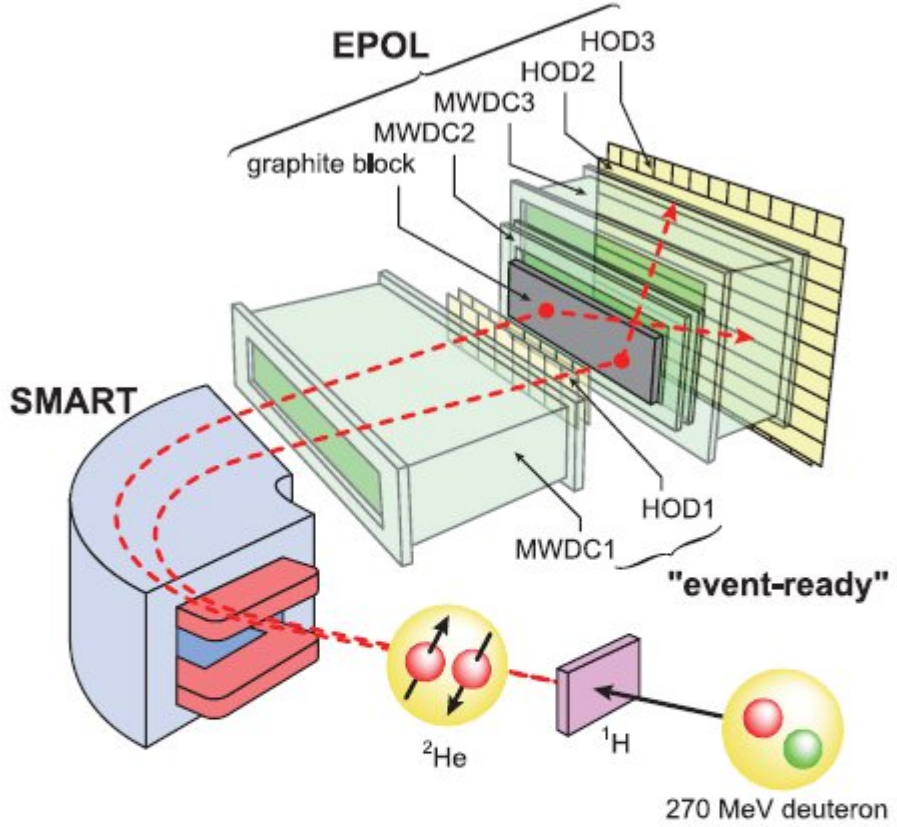

FIG. 1 (color). A schematic diagram of the experimental layout. Deuterons interact with protons in liquid hydrogen (^{1}H) target. The proton pairs (^{2}He) are momentum selected by SMART spectrometer, which are subsequently tracked by the “event-ready” detector (MWDC1 and HOD1). The spin analysis of the protons was then achieved by the EPOL polarimeter, where graphite block is the analyzer and the MWDC2, MWDC3, HOD2, and HOD3 are correlation detectors.

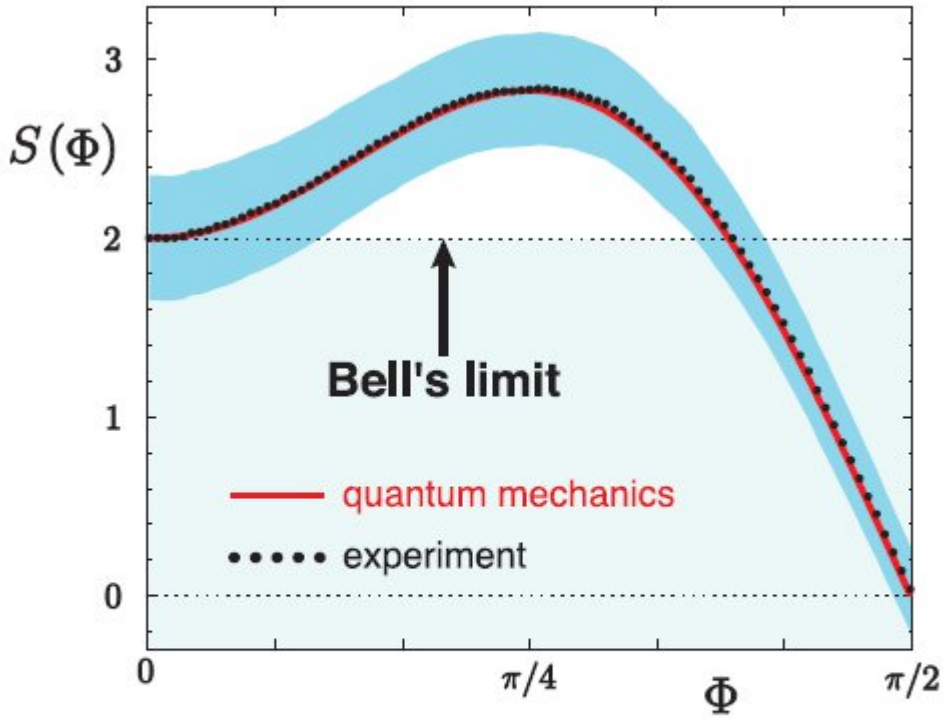

FIG. 4 (color). Plot of the spin-correlation function $S(\Phi)$ vs Φ. Solid circles are the experimental result $S_{\rm exp}(\Phi)$ derived from the same data set. Each error shown as blue shaded area is correlated. See text for details.

^{16}Ne = ^{14}O + 2p

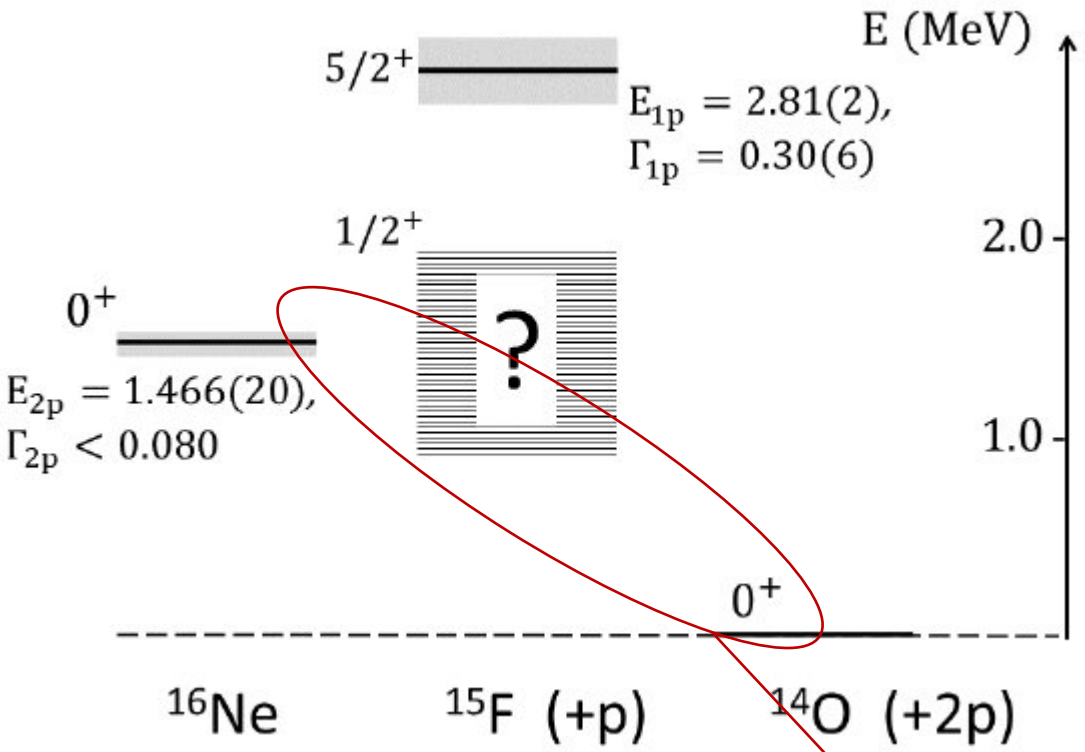

TABLE II. Core-proton $s_{1/2}$ and $d_{5/2}$ resonances of the ^{15}F $= {}^{14}$O$+p$. The unit is MeV.

^{15}F	$E_p(s_{1/2})$	$\Gamma_p(s_{1/2})$	$E_p(d_{5/2})$	$\Gamma_p(d_{5/2})$
Expt.[21]	1.23(5)	0.50-0.84	2.81(2)	0.30(6)
[20]	1.23-1.37	0.7	2.795(45)	0.325(6)
	1.35-1.61	–		
[19]	1.51(15)	1.2	2.853(45)	0.34
[18]	1.47(13)	1.0(2)	2.77(10)	0.24(3)
prompt	$\cong$ 1.5	$\cong$ 1.3	2.785	0.391
mixed	1.277	0.604	2.787	0.264

Core-proton potential is adjusted to reproduce these 1p-energy and width.

$$\hat{h}(r_i) = -\frac{\hbar^2}{2\mu}\frac{d^2}{dr_i^2} + V(r_i),$$

$$V(r_i) = \frac{\hbar^2}{2\mu}\frac{l(l+1)}{r_i^2} + V_{WS}(r_i) + V_{Coul}(r_i),$$

If the intermediate $s_{1/2}$ resonance in ^{15}F exists, the sequential 1p-1p emission can take place.

^{16}Ne = ^{14}O + 2p: spin correlation

Preliminary

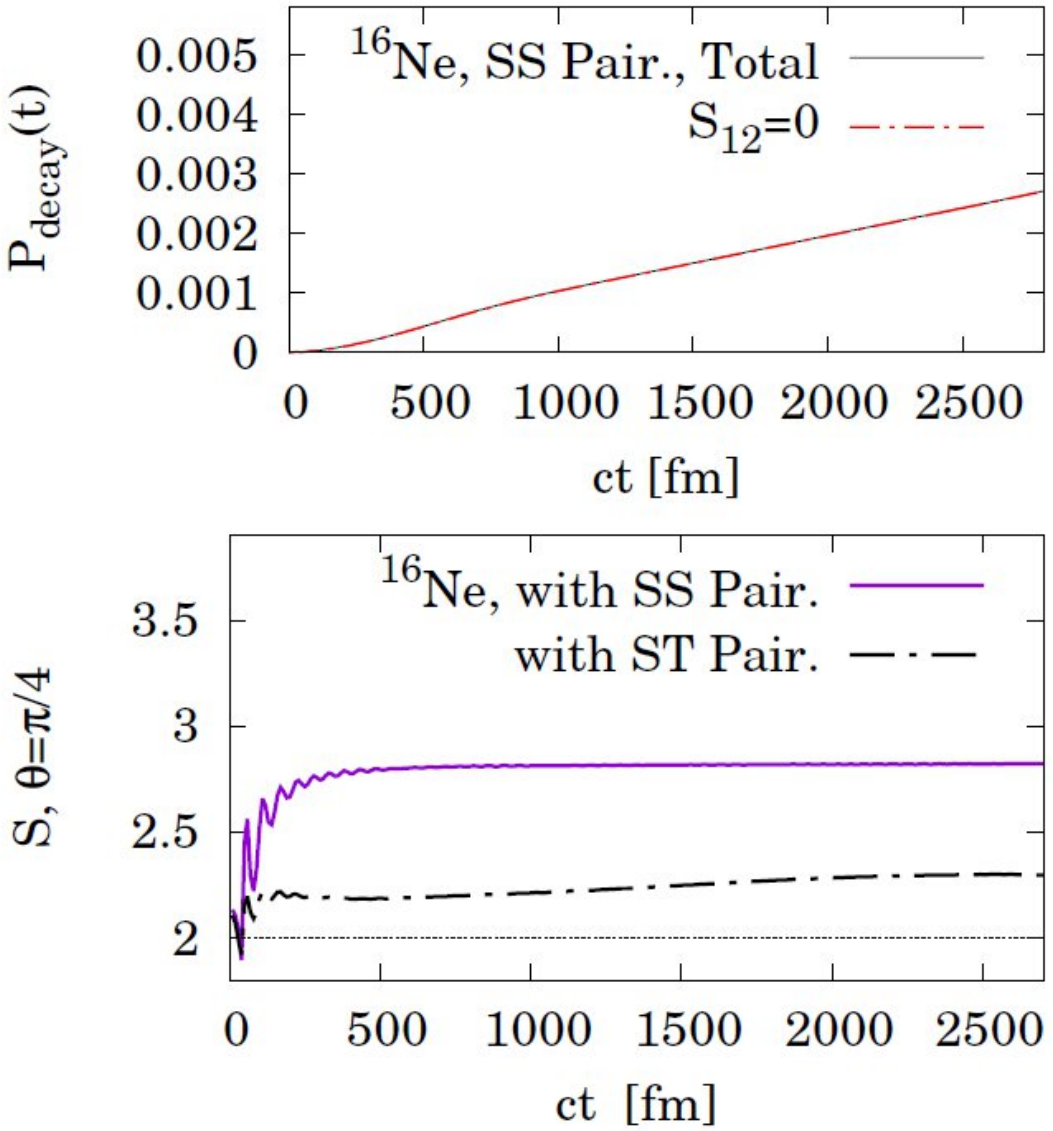

$$P_{decay}(t) \equiv \iint |\psi_{dcy}(t, r_1, r_2)|^2 \, dr_1 dr_2 = \langle \psi_{dcy}(t) \mid \psi_{dcy}(t) \rangle \,,$$
$$= \cdots = 1 - |\langle \psi(0) \mid \psi(t) \rangle|^2 \,.$$

$$S = \max \{ |S_{-+++}| \,, |S_{+-++}| \,, |S_{++-+}| \,, |S_{+++-}| \} \,, \quad (5)$$

where

$$S_{-+++} = -\langle A_1 B_1 \rangle + \langle A_2 B_1 \rangle + \langle A_1 B_2 \rangle + \langle A_2 B_2 \rangle \,,$$
$$S_{+-++} = \langle A_1 B_1 \rangle - \langle A_2 B_1 \rangle + \langle A_1 B_2 \rangle + \langle A_2 B_2 \rangle \,,$$
$$S_{++-+} = \langle A_1 B_1 \rangle + \langle A_2 B_1 \rangle - \langle A_1 B_2 \rangle + \langle A_2 B_2 \rangle \,,$$
$$S_{+++-} = \langle A_1 B_1 \rangle + \langle A_2 B_1 \rangle + \langle A_1 B_2 \rangle - \langle A_2 B_2 \rangle \,. \quad (6)$$

^{16}Ne (0^+)	E_{2p} [MeV]	Γ_{2p} [MeV]	S_{CHSH}
This work (SS)	1.404	1.4 x 10^{-4}	2.81
Expt.	1.466(20)	(< 0.08)	?

Ⓟ A spin correlation beyond the LHV-theory limit is predicted.
Ⓟ This correlation is sensitive to the 2p interaction. [SAME to ^{6}Be]

Experimental Setup

AIM: Check violation of CHSH inequality for intrinsic spin correlation, considering total momentum conservation, gs in 16Ne and orientation after transfer

17Ne(3He,4He)16Ne → 14O+p+p

Beam 17Ne ~10E5, 10 MeV/A

- Analyze angular distributions for different L values
- Extract correlations between s1_z, s2_z projections for each L
- VAMOS: measure 14O (or 15F) ions
- GRIT: measure proton correlations
- AGATA: measure decay radiation to 14O, (narrow) resonances?